

Copyright page:

©2012  
David A Grunat

ALL RIGHTS RESERVED

Effects of soil saturation and pore fluid salinity on complex conductivity

by

David A Grunat

A Dissertation submitted to the

Graduate School-Newark

Rutgers, The State University of New Jersey

in partial fulfillment of the requirements

for the degree of

Master of Science

Graduate Program in Environmental Geology

written under the direction of

Lee D. Slater

and approved by

---

---

---

Newark, New Jersey

January 2013

## **ABSTRACT OF THE DISSERTATION**

Improved understanding on the effects of soil saturation on spectral induced polarization

By David A Grunat

Dissertation Director:  
Lee D. Slater

Recent studies have shown that induced polarization (IP) coupled with electrical resistivity surveys can be used for in-situ lithological and hydrologic discrimination of the subsurface; yet the driving factors behind the effects of water content dynamics on IP are relatively understudied. We sought to improve understanding of the relationship of IP on variations in saturation state for an undisturbed agricultural soil. Our experiment consisted of collecting IP measurements concurrently with hydraulic data during multistep outflow experiments. We determined the hydraulic properties of the undisturbed soil samples and correlated them with IP data, primarily changes in saturation. Due to an increase in salinity with decreasing saturation, we found that imaginary conductivity ( $\sigma''$ ) may offer distinct advantages for determining moisture content over real conductivity ( $\sigma'$ ) measurements. Although  $\sigma''$  exhibits a weaker dependence on saturation compared to  $\sigma'$ , the relative insensitivity of  $\sigma''$  to salinity creates a more robust measure of moisture content in the presence of changing salinities. As changes in pore fluid conductivity are likely to occur in the field simultaneously with water content changes, we argue that, although IP has traditionally been used to discriminate lithology, temporal IP measurements may additionally provide a robust indicator of changes in saturation state.

## **Acknowledgement**

I would like to thank the people who have helped me during my Master's Program.

Firstly I would like to thank my advisors. Dr. Markus Wherer, who provided me with much assistance throughout my Master's studies. This research would not have been possible without his insight including: helping me with experimental setup, data analysis, and presentation. Dr. Lee Slater who not only provided insight on the research but also helped me to be successful with my graduate studies. Finally, Dr. Daniel Gimenez who provided a non-geophysics look at my findings and helped me to understand the unsaturated dynamics of my experiments.

I would also additionally like to thank those who assisted with my research. These people include Rutgers University students Samayra Vincent and Sundeep Sharma for their assistance with building the experimental setup and data collection. The many people at the Cornell Cooperative Extension for allowing for and assisting with soil collection. The chair of hydrogeology, University of Jena for providing soil physical analysis beyond what our lab was capable of conducting. I would also like to thank Liz Morrin of Rutgers Department of Earth and Environmental Sciences for all her assistance from helping with paperwork and orders to just being someone to talk to.

Finally, I would like to thank all of my friends and family for their support through my studies. While at times I didn't think that finishing was possible they always provided me with support and reassurance I would succeed. I would especially like to thank my

partner Sara Carbone as if it was not for her, I would never had been able to attend or survive graduate school.

This research was made possible by the support of the Geological Society of America (GSA) through the student research grant program and the Allan V. Cox Student Scholarship Award Fund and the Deutsche Forschungsgemeinschaft (DFG; Grant number WE 4979/1-1).

## Table of Contents

<b>ABSTRACT OF THE DISSERTATION .....</b>	<b>II</b>
<b>ACKNOWLEDGEMENT .....</b>	<b>III</b>
<b>TABLE OF CONTENTS .....</b>	<b>V</b>
<b>LIST OF TABLES.....</b>	<b>VI</b>
<b>LIST OF ILLUSTRATIONS .....</b>	<b>VII</b>
<b>INTRODUCTION .....</b>	<b>1</b>
<b>ELECTRICAL PROPERTIES.....</b>	<b>4</b>
<b>HYDRAULIC THEORY .....</b>	<b>9</b>
<b>METHODS.....</b>	<b>10</b>
SAMPLE COLLECTION AND COLUMN CONSTRUCTION .....	10
MULTI-STEP OUTFLOW EXPERIMENT .....	14
ARCHIE EXPERIMENT .....	16
<b>RESULTS .....</b>	<b>17</b>
REAL CONDUCTIVITY .....	21
IMAGINARY CONDUCTIVITY .....	26
<b>DISCUSSION .....</b>	<b>27</b>
<b>CONCLUSION.....</b>	<b>31</b>
<b>REFERENCES.....</b>	<b>32</b>
<b>CURRICULUM VITAE.....</b>	<b>38</b>

## List of Tables

**Table 1)** *Physical Properties for Haven Loam Soil from Cornell Cooperative Extension, Riverhead, New York*

**Table 2)** *Hydrus-1D Boundary Conditions and Experimental Parameters for Multi-Step Outflow Experiments on Column 1 (a) and Column 2 (b)*

**Table 3)** *Hydrus-1D inverse solution showing parameter estimation and standard error for Column 1 (a) and Column 2 (b)*

**Table 4)** *Parameter estimation for real conductivity accounting for ion release (Eq. [18]) and no ion release (Eq. [10]) for Column 1 no flow (a) and Column 2 no flow (b) with root mean square errors (RMSE)*

**Table 5)** *Parameter estimation for power law relationship of imaginary conductivity with saturation (Eq. [9]) for Column 1 no flow (a) and Column 2 no flow (b)*

## List of illustrations

**Figure 1)** Schematic of idealized behavior of cations with and without electric current.

**Figure 2)** Column construction showing the electrode and tensiometers locations (a), electrode construction (b), and connection to digital signal analyzer (c).

**Figure 3)** (a) Observed outflow versus Hydrus modeled outflow, (b) Observed average water content and modeled water content at lower tensiometers including sensitivity analysis varying estimated parameters ( $\alpha$ -1,  $\alpha$ -2, n-1 and n-2) by  $\pm 10\%$  in Column 1 No Flow.

**Figure 4)** IP results at 1 Hz during multi-step outflow experiment showing real conductivity ( $\sigma'$ ), imaginary conductivity ( $\sigma''$ ) and phase shift ( $\phi$ ) for Column 1 Flow (a), Column 1 No Flow (b), Column 2 Flow (c), and Column 2 No Flow (d), imaginary conductivity scaled by 1000.

**Figure 5)** SIP results for Column 1 during multi-step outflow experiment showing frequency dependence of real conductivity ( $\sigma'$ ) and imaginary conductivity ( $\sigma''$ ) and line indicating 1 Hz frequency used for single frequency analysis, imaginary conductivity scaled by 1000

**Figure 6)** Real ( $\sigma'$ ) and Imaginary Conductivity ( $\sigma''$ ) versus pore fluid conductivity ( $\sigma_w$ ) showing a linear relationship for real conductivity in Column 1 (a) and Column (2) (b) and a weaker dependence of imaginary conductivity

**Figure 7)** (a) Real conductivity ( $\sigma'$ ) versus saturation showing modeled fits accounting for ion release and not accounting for ion release using constant pore fluid conductivity in Column 1 during no flow conditions. (b) Imaginary conductivity ( $\sigma''$ ) versus saturation in Column 1 during no flow conditions showing a power law relationship.

**Figure 8)** Similarity between imaginary conductivities ( $\sigma''$ ) versus saturation in all four datasets with power law relationship shown (a) compared to dissimilarities between real conductivities ( $\sigma'$ ) versus saturation in all four datasets (b)



## **Introduction**

Electrical methods are an emerging technology in the field of soil sciences, offering the opportunity to observe in-situ spatial and temporal variations in subsurface properties including spatial heterogeneity of soil matrix and hydraulics where traditional data collection only provides point measurements (Hubbard and Rubin, 2000). In addition, these techniques provide data collection with minimal disturbance and associated costs. The use of electrical resistivity for the characterization of moisture and pore water quality dynamics has been extensively explored (see Lesmes and Friedman (2005), for review).

Electrical resistivity has been used for subsurface imaging due to its dependence on salinity, soil structure and degree of saturation (Archie, 1942). Archie's Law has been utilized in the interpretation of resistivity data for decades. One use of Archie's Law is the determination of moisture content, or its changes, in the vadose zone. However, while resistivity is strongly dependent on saturation, the additional dependence on salinity and soil structure can often limit the interpretation of data. Time-lapse resistivity surveys can be used to isolate resistivity changes with time associated with moisture dynamics (Mitchell et al., 2011). While this method removes the effects of lithology, linking changes in moisture content to resistivity can be complicated by temporal changes in salinity.

While moisture content, salinity, and soil matrix changes can be difficult to discriminate in resistivity surveys in the absence of additional information, recent studies have shown that induced polarization surveys can be used to discriminate resistivity changes

associated with pore fluid variations from resistivity changes associated with physical properties, e.g. surface area and hydraulic conductivity (Kemna et al., 2000; Slater and Lesmes, 2002). While a relatively weak dependence of induced polarization (compared to resistivity) on moisture content is known, how unsaturated water content dynamics affect induced polarization measurements remains relatively understudied (Breede et al., 2011; Schmutz et al., 2010; Titov et al., 2004; Ulrich and Slater, 2004).

While many studies have been conducted using resistivity, relatively few studies have investigated the effects of saturation state on induced polarization. An early investigation on saturation effects was conducted by Vinegar and Waxman (1984) using oil as a non-wetting fluid in shaly sand samples. They observed decreases in real conductivity ( $\sigma'$ ) and imaginary conductivity ( $\sigma''$ ) with decreasing saturation that could be well described by a power law relationship. The power-law exponent for  $\sigma''$  ( $p$ ) was determined to be lower than the power law exponent for the real conductivity  $\sigma'$  ( $n$ ), following the relationship  $p=n-1$ . Schmutz et al. (2010) conducted IP measurements on sands using oil as a non-wetting fluid and also observed decreasing  $\sigma''$  with increasing saturation that could be described by a power law relation. Ulrich and Slater (2004) conducted IP measurements on sand samples under evaporative drying and also observed power law relationships where  $p < n$ . However, Ulrich and Slater (2004) also conducted measurements using pressure drainage and inhibition where a peak in  $\sigma''$  was observed during desaturation. Breede et al. (2011) conducted IP measurements on both sands and a laboratory packed agricultural sample. They also observed a peak in  $\sigma''$  during desaturation followed by a decrease in  $\sigma''$ . In general, these studies generally suggest that

$\sigma''$  decreases with decreases in saturation, with Vinegar and Waxman (1984), Ulrich and Slater (2004), and Schmutz et al. (2010) demonstrating a weaker power law relationship of  $\sigma''$  as compared to the relationship for  $\sigma'$ .

Two recent theoretical models have been proposed to describe changes in water content on the observed IP response. The first relates the response of  $\sigma''$  to a ratio between large and narrow passages for current flow (Titov et al., 2002). Using this theory, Titov experimentally demonstrated an increase in  $\sigma''$  in unconsolidated sands to some peak level associated with a peak ratio of large and narrow water filled pore diameters, followed by a decrease (Titov et al., 2004). This model is consistent with the peak  $\sigma''$  values seen by other researchers (Breede et al., 2011; Titov et al., 2004; Titov et al., 2002; Ulrich and Slater, 2004). Additionally, this model may explain the lack of a peak during evaporative drying as all pores simultaneously drain (Ulrich and Slater, 2004) or when a highly heterogeneous soil is used due to the superposition of multiple peaks. The second model initially presented by Leroy and Revil (2009) for saturated conditions, attributes induced polarization to the polarization of the Stern layer around soil particles that is discontinuous within the porous media. Jougnot et al. (2010) refined this relationship to account for changes in saturation by modifying the charge density of counterions per unit pore volume with varying saturation. Experimentally, they demonstrated a decrease in  $\sigma''$  with decreasing saturation (Jougnot et al., 2010). This model does account for the general power law decrease in  $\sigma''$  with decreases in saturation, but is unable to describe the peak values observed by others.

The original objective of this study was to collect and correlate IP data with observed hydraulic properties and to further investigate the dependence of IP on saturation state. We performed laboratory experiments to investigate the effects of IP during water desaturation on undisturbed loamy sediments from an agricultural site. To our knowledge, no previous IP studies have been conducted on undisturbed soil columns and none have been conducted under field conditions. Measurements were conducted under flow and no flow conditions using pore fluids of similar salinity as observed in agricultural soils (Blume et al., 2010). Due to an observed increase in pore fluid conductivity during desaturation, we observed and modeled changes in complex conductivity as a function of both pore fluid conductivity and saturation. We present evidence that imaginary conductivity is a more robust sensor of changes in saturation state than real conductivity under conditions of changing pore fluid salinity.

### **Electrical Properties**

Spectral induced polarization (SIP) measurements are conducted by injecting current over a range of frequencies, with a phase lag ( $\varphi$ ) and magnitude ( $|\sigma|$ ) of the voltage waveform observed between electrodes measured. These results can be presented as magnitude and phase or can be reported in terms of an in-phase real conductivity ( $\sigma'$ ) representing electromigration and an out of phase imaginary conductivity ( $\sigma''$ ) representing polarization. Using the measured phase lag and magnitude,  $\sigma'$  and  $\sigma''$ , the following relationships hold,

$$|\sigma| = \sqrt{(\sigma')^2 + (\sigma'')^2}, \quad (1)$$

$$\varphi = \tan^{-1} \left( \sigma' / \sigma'' \right), \quad (2)$$

$$\sigma' = |\sigma| \cos \varphi, \quad (3)$$

and

$$\sigma'' = |\sigma| \sin \varphi. \quad (4)$$

Vinegar and Waxman (1984) developed a model to describe the complex conductivity ( $\sigma^*$ ) of shaly sandstone. Their model consists of the parallel addition of the electrolytic contribution ( $\sigma_{el}$ ) representing electromigration through the interconnected pore space and a mineral surface contribution consisting of both electromigration ( $\sigma'_{surf}$ ) and polarization ( $\sigma''_{surf}$ ) through the electrostatic double layer (EDL). The Vinegar and Waxman (1984) model assumes the following equations:

$$\sigma^* = \sigma_{el} + \sigma^*_{surf}, \quad (5)$$

and

$$\sigma^* = (\sigma'_{el} + \sigma'_{surf}) + i\sigma''_{surf}. \quad (6)$$

As shown in the above equations,  $\sigma''$  depends only on the surface polarization while  $\sigma'$  depends on both electrolytic and surface conduction. Archie's Law is commonly used to describe electrolytic conduction in porous media,

$$\sigma_{el} = \frac{1}{F} \sigma_w S_w^n = \sigma_w \varphi^m S_w^n \quad (7)$$

where  $F$  (-) is the formation factor,  $\sigma_w$  ( $\text{S m}^{-1}$ ) is fluid conductivity,  $\phi^m$  (-) is porosity raised to Archie's cementation factor  $m$  (-), and  $S_w$  is saturation ( $S_w = \theta/\phi$ , where  $\theta$  (-) is the water content) raised to Archie's saturation factor  $n$  (-) (Archie, 1942). Archie's cementation factor ( $m$ ) can be used to describe the effects of intergranular cementation and grain shape with typical values of 1.3 for clean sand to 4.4 for Mexican Altered Tuff (a clay rich mineral) with a heterogeneous soil material exhibiting a cementation factor of approximately 2 (Lesmes and Friedman, 2005). Archie's saturation factor is typically reported as approximately 2 for unconsolidated sediments with experimental results showing it ranging from 1.3 to 2.7 (Schön, 2004). Using this relationship the electrical resistivity is commonly used to estimate moisture content.

As previously discussed  $\sigma'$  depends on both electrolytic and surface conductivity and using the Vinegar and Waxman (1984) parallel conductor model,  $\sigma'$  can be described under saturated conditions using the following relationship:

$$\sigma' = \frac{1}{F} \sigma_w + \sigma'_{surf} \quad (8)$$

where  $F$  is independent of  $\sigma_w$  and thus  $\sigma'$  varies linearly as a function of salinity. Using Archie's law (Eq. [7]), the soil porosity and formation factor can be used to determine Archie's cementation factor at full saturation (i.e.  $S_w=1$ ). Additionally, surface conduction ( $\sigma'_{surf}$ ) can be determined as the residual conduction at low salinities.

Imaginary conductivity represents the ability of a soil to polarize from the presence of interfaces at which local charge concentration gradients form upon application of electrical current. Charges at a particle surface result in an interfacial region of counterions necessary to provide equilibrium in a solution. This interfacial zone of charge is typically referred to as the electrical double layer (EDL). As distance from the particle surface increases the charge density decreases. Two distinct zones can be derived, the first being the “Stern” layer described as the zone near the surface where ions are strongly bound. The outer layer is known as the “diffuse” layer where ions are less strongly bound and ion exchange can occur (Hillel, 2004). A schematic of the idealized behavior of cations in the stern layer with and without an electric current is presented as Figure 1.

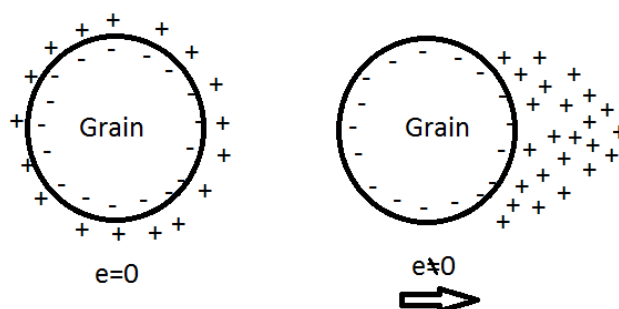


**Figure 1)** Schematic of idealized behavior of cations with and without electric current.

The redistribution of cations in the EDL in the presence of electrical current and subsequent relaxation when the electrical current is removed is the basis for IP measurements.

Previous research has shown that the magnitude of this polarization is dependent on

surface area, surface charge density, surface ionic mobility and surface tortuosity (Frye et al., 1998; Glover, 1998; Revil and Florsch, 2010; Revil et al., 1999; Schön, 2004).

Additionally, it has been shown that  $\sigma''$  in saturated samples is sensitive to salinity changes; with a power law increase of  $\sigma''$  with increases in salinity to some critical salinity where  $\sigma''$  becomes asymptotic around  $1 \text{ S m}^{-1}$  (Flath, 1989; Slater and Glaser, 2003; Vinegar and Waxman, 1984; Weller et al., 2011). This weak dependence of  $\sigma''$  on fluid chemistry has motivated the use of IP methods for improving lithologic discrimination relative to using resistivity alone (Weller et al., 2011; Weller and Slater, 2012; Weller et al., 2010).

As previously discussed,  $\sigma''$  typically exhibits a power law relationship with changes in saturation:

$$\sigma'' = a S_w^p \quad (9)$$

where  $a$  is a fitting parameter (Su et al., 2000; Ulrich and Slater, 2004). As previously discussed, Vinegar and Waxman (1984) proposed  $p=n-1$  describing the effects of oil on shaly sands. Although Ulrich and Slater determined no correlation between sediment structure and  $p$ , they did observe that  $p$  was consistently less than Archie's Saturation factor  $n$ . Furthermore, Schmutz et al. (2010) additionally discussed the power law relationship; similar to Vinegar and Waxman (1984), they fit  $p$  as a function of  $n$  where it was assumed that  $p=n-1$  (Schmutz et al., 2010).



To compare the real and imaginary parts of the complex surface conductivity, Börner (1991, 1992) demonstrated experimentally a linear proportionality of  $\sigma'_{surf}$  and  $\sigma''_{surf}$ . Assuming this linear relationship can be extended to changes in saturation, we similarly assume real surface conduction varies linearly with surface polarization by constraining  $\sigma'_{surf}$  by  $S_w^p$  resulting in:

$$\sigma' = \sigma_w \phi^m S_w^n + \sigma'_{surf} S_w^p \quad (10)$$

### Hydraulic Theory

Flow through unsaturated media can be described by a modification of Darcy's law (Darcy, 1856) known as Richards' Equation (Richards, 1931):

$$\frac{\partial \theta}{\partial t} = \frac{\partial}{\partial z} \left[ K(\theta) \frac{\partial h}{\partial z} - K(\theta) \right] \quad (11)$$

where  $\theta$  (-) is volumetric water content,  $K$  ( $L T^{-1}$ ) is hydraulic conductivity,  $t$  (T) is time, and  $z$  (L) is length (Durner et al., 1999). Durner et al. (1999) revised Van Genuchten's model (van Genuchten, 1980) to describe the water retention curve and unsaturated conductivity for multimodal pore-size distributions using a linear superposition of van Genuchten models:

$$S_w(h) = \frac{\theta - \theta_r}{\theta_s - \theta_r} = \frac{\sum_{i=1}^k w_i [1 + (\alpha_i |h|)^{N_i}]^{-m_i}}{1} \quad \begin{matrix} \text{for } h < 0 \\ \text{for } h \geq 0 \end{matrix} \quad (12)$$

$$K(S_w) = \frac{\sum_{i=1}^k (w_i S_{wi})^\tau \left( \sum_{i=1}^k w_i \alpha_i \left[ 1 - \left( 1 - S_{wi}^{1/m_i} \right)^{m_i} \right] \right)^2}{\sum_{i=1}^k w_i \alpha_i} \quad (13)$$

where  $k$  (-) is the number of pore-sizes present,  $\tau$  (-) is an empirical shape parameter,  $w_i$  are weighting factors where  $0 < w_i < 1$  and  $\sum_{i=1}^k w_i = 1$ , and  $\alpha_i$ ,  $N_i$  and  $m_i$  are fitting parameters for each pore size distribution (Durner et al., 1999). This relationship for two pore size distributions is referred to as the dual van-Genuchten-Mualem model.

## Methods

### Sample Collection and Column Construction

Samples analyzed for this experiment were from an agricultural soil collected from the Cornell Extension Cooperative in Riverhead, New York on Long Island, where geophysical methods are being used to better understand the transport of fertilizers and pesticides through the vadose zone. Two samples were collected by driving a sharpened PVC column into undisturbed soil in adjacent locations. Each sample was capped in the field and stored in a cool (10°C) and dark environment prior to analysis to prevent soil structure changes due to temperature and humidity changes and to limit microbial growth. Soil physical properties were determined including grain size distribution by sieving and sedimentation. Bulk density and porosity were determined by calculating the saturated and dry mass of soil. Surface area for the soil was determined by using the Nitrogen Brunauer-Emmett-Teller (BET) adsorption method (Micromeritics ASAP 2020, Norcross, GA, US). For determination of the cation exchange capacity the samples were first treated with 0.1 M and 2.5 mM BaCl<sub>2</sub> followed by 0.02 M MgSO<sub>4</sub>. The

concentration of exchanged Mg was measured by ICP-OES (Varian 725 OES, Varian, Germany). Organic carbon content was determined by oxidative combustion of 100 to 200 mg air-dried, homogenized sample material in a high temperature furnace at 1300 °C with subsequent NDIR detection of the resulting CO<sub>2</sub> on a multi N/C 2100 (Analytic Jena, Jena, Germany). Soil physical properties for the agricultural soil are presented in Table 1.

**Table 1)** Physical Properties for Haven Loam Soil from Cornell Cooperative Extension, Riverhead, New York

<b>Sand</b>	<b>Silt</b>	<b>Cla</b>	<b>Bulk Density</b>
<i>(%)</i>	<i>(%)</i>	<i>(%)</i>	<i>(g cm<sup>-3</sup>)</i>
41.40±1.07	52.45±0.68	6.15±0.40	1.65
<b>Porosity</b>	<b>Nitrogen BET Surface Area</b>	<b>Cation Exchange Capacity</b>	<b>Organic Carbon Content</b>
<i>(%)</i>	<i>(m<sup>2</sup>/g)</i>	<i>(meq kg<sup>-1</sup>)</i>	<i>(g kg<sup>-1</sup>)</i>
38	8.47±0.04	31±3	6.72±0.08

Two measurement columns were constructed using 2-inch diameter by 10-inch clear schedule-40 PVC pipe and non-conductive PVC fittings (Figure 2). Each column consisted of eight electrodes, two tensiometers, and a porous plate. The electrodes were constructed using 12-gauge non-polarizing silver-silver chloride (Ag-Ag/Cl) wire in a 0.1 M KCl electrolyte solution connected to the soil with porous ceramic cups (1 bar air entry pressure, Sunvalley Solutions, Sunny Isles Beach, FL, US) to retain electrolytic contact during soil desaturation and to prevent anomalous phase results. Through this

electrolytic contact, the electrodes resulted in a pore fluid conductivity variation that will be further described below.

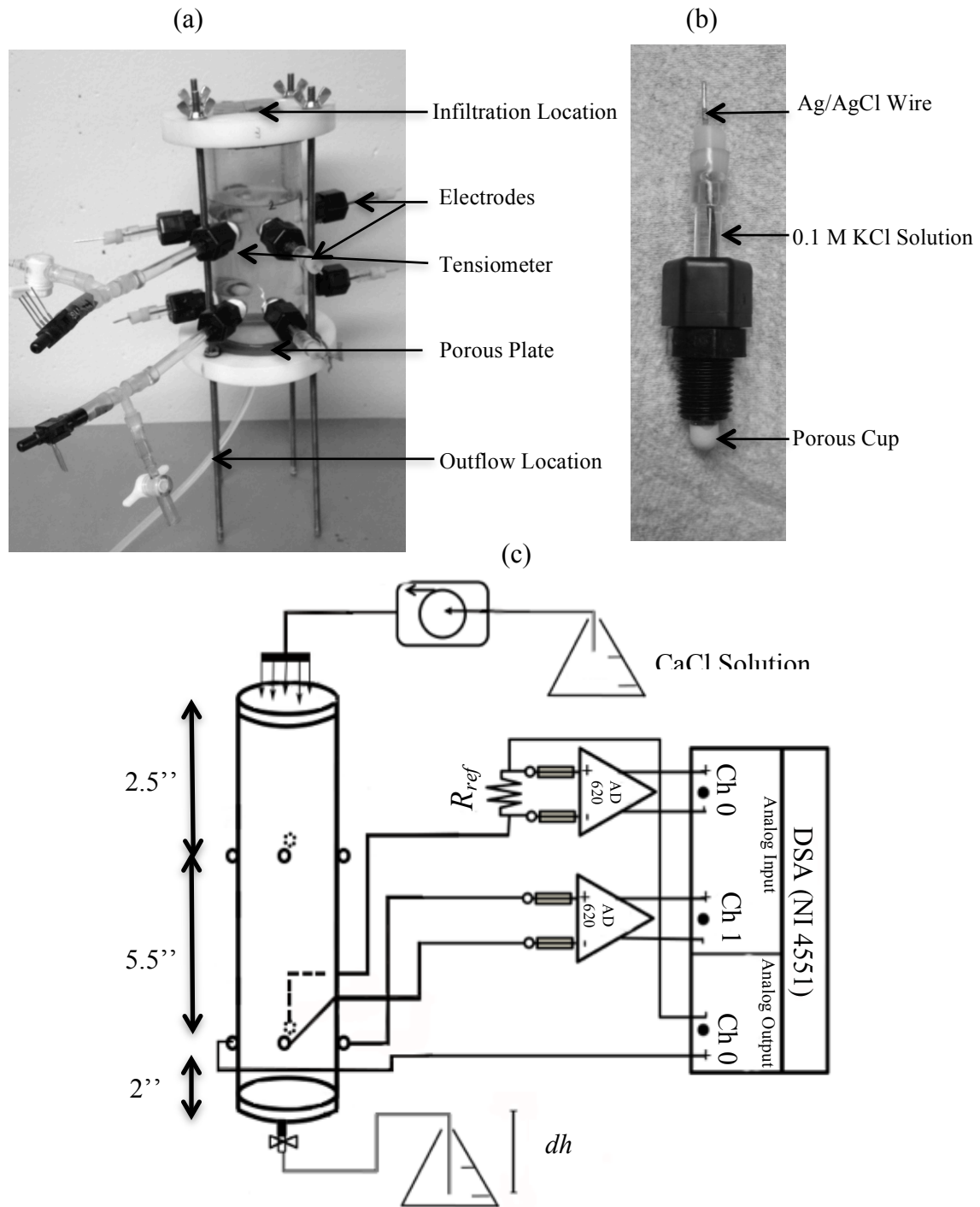


**Figure 2)** Column construction showing the electrode and tensiometers locations (a),

electrode construction (b), and connection to digital signal analyzer (c).

For this experiment, four electrodes organized in a horizontal plane were utilized, as vertically separated electrodes would integrate over a range of moisture contents due to the vertical distribution of moisture content associated with gravity. SIP measurements were collected by using four electrodes 2-inches above the bottom of the column connected to a digital signal analyzer (NI4551 DSA, National Instruments, Austin, TX, US). Initially measurements were collected using both upper and lower electrodes; however, due to the time required for data collection only one plane could be collected through each experiment. The bottom electrodes were selected as infiltrating pore fluid during flow conditions could create an anomalous increase in saturation near the upper electrodes. Measurements were collected over 40 equally spaced frequency intervals between 0.1 and 1000 Hz. Impedance magnitude and phase shift were measured relative to a precision resistor using opposite electrodes on the horizontal plane to the current electrodes. During column calibration, the column was filled with water of varying salinities. Both traditional vertical electrode arrays and horizontal arrays were tested to ensure reliability of the horizontal data by reproducing the vertical data. The geometric factor, which is a correction factor used to convert an apparent conductivity (a function of the electrode locations) to a true conductivity (assuming homogeneity with the support volume) for electrodes in different arrays, is often determined by measuring the distances between current and potential electrodes for one-dimensional current flow along a column. Due to the close proximity of the electrodes and three-dimensional flow from point electrodes preventing a simple analytical solution for the geometric factor, the

horizontal electrode array was calibrated experimentally using fluids of known conductivity ranging from approximately 50 to 3000  $\mu\text{S cm}^{-1}$ . Linear regression of resistance against known sample resistivity resulted in a coefficient of determination ( $R^2$ ) of 99%; phase errors were less than 1 mrad below 10 Hz. As we focus on a single frequency of 1 Hz, this was deemed suitable for these measurements. Additionally, prior to sample analysis, saturated measurements were conducted on laboratory grade Ottawa sand to ensure a typical SIP response was achieved and no artifacts from the non-traditional horizontal array were present.

Two tensiometers were placed in the plane bounded by both the upper and lower electrode arrays for continuous tension measurements. Tensiometers were constructed by connecting pressure transducers (26PCCFA6D, Honeywell, Morristown, NJ, US), to a small column of degassed deionized water connected to the soil with Sunvalley Solutions porous ceramic cups. The porous plate placed beneath the soil was constructed using a membrane disc filter (3.0  $\mu\text{m}$  Versapor, Pall Corporation, Port Washington, NY, US), affixed to a polyethylene disk. Air entry values were tested and determined to be greater than 3 meters and thus deemed suitable for these experiments as the maximum suction head applied was 3 meters. The entire column was placed on a balance to continuously record water content changes via weight loss.

### **Multi-Step Outflow Experiment**

A widely accepted method for determination of unsaturated hydraulic parameters is the use of a multistep outflow experiment (Vereecken et al., 1997). This method is based on the measurement of the diminishing outflow from samples in a column after suction at

the lower boundary is changed by a measured increment. By using in-situ measurements of tension to determine a gradient and measurement of overall moisture content, the  $K(S_w)$  and  $K(h)$  relationship can be modeled for a range of moisture contents (Hillel, 2004).

Two multi-step outflow experiments were conducted on each of two soil columns by applying suction at the lower boundary with hanging water column. The first experiment consisted of applying a constant flux of  $380 \mu\text{S cm}^{-1}$   $\text{CaCl}_2$  pore fluid at  $0.3 \text{ mm hr}^{-1}$  while lowering the suction at the lower boundary to decrease water content (Table 2). A  $380 \mu\text{S cm}^{-1}$  solution was chosen based on the median value of typical pore fluid conductivities in agricultural soils (Blume et al., 2010).  $\text{CaCl}_2$  was used to prevent dispersion of the fine-grained sediments altering the physical properties of the soil. The second experiment consisted of starting with the column fully saturated with  $380 \mu\text{S cm}^{-1}$   $\text{CaCl}_2$  pore fluid and lowering the suction at the lower boundary to decrease water content with no additional influx of pore fluid. Prior to initial measurements the columns were flushed with fresh pore fluid for approximately 2 weeks to prevent influence of 'first flush' behavior (Wehrer and Totsche, 2009) associated with the exchange of naturally present ions with the  $\text{CaCl}_2$  used during the laboratory experiments.

Using the multi-step outflow data, an inverse model was created using Hydrus-1D (Šimůnek et al., 2008). We first attempted to fit a single van-Genuchten model but this was unable to sufficiently model the data. Therefore, a dual-porosity inverse model was used to determine the coefficients necessary for a dual van-Genuchten-Mualem model as

proposed by Durner et al. (1999) (Eq. [12]). The boundary conditions and parameters of the simulation are presented in Table 2.

**Table 2)** Hydrus-1D Boundary Conditions and Experimental Parameters for Multi-Step Outflow Experiments on Column 1 (a) and Column 2 (b)

<b>(a)</b>		<b>(b)</b>	
<b>Elapsed Time (Hours)</b>	<b>Boundary Condition Suction at Lower Boundary (cm)</b>	<b>Elapsed Time (Hours)</b>	<b>Boundary Condition Suction at Lower Boundary (cm)</b>
6.5	0	23.65	0
24.62	-10	23.75	-10
48.5	-40	120.75	-40
74.74	-80	166.75	-80
192	-100	191.75	-120
241	-319	289.00	-312

Based on the soil physical properties  $\theta_s$  was set at 0.38 equal to porosity,  $\theta_r$  was set at 0.001, and the tortuosity parameter  $I$  was left at the default value of 0.5. Using the early outflow conditions and tensions at low suctions and late outflow conditions at higher suctions a single van-Genuchten model was used to model individually the early and late data. The individual results were then used as initial guesses for the dual porosity inverse solution.

### Archie Experiment

To evaluate the Archie's Formation Factor ( $F$ ) and the contribution of surface conduction ( $\sigma'_{surf}$ ) in each column, an Archie experiment was conducted by measuring  $\sigma'$  while varying salinity under saturated conditions. Prior to collecting measurements, the column



was again flushed with deionized water for approximately two weeks to prevent ‘First Flush’ behavior from the exchange of ions from the soil. The column was then flushed with pore fluids with salinities ranging from approximately 0.85 to 1000  $\mu\text{S cm}^{-1}$ . For each salinity interval, the column was flushed from below for 24 hours prior to measurement. A linear regression of pore fluid salinity and  $\sigma'$  was conducted to determine the formation factor and contribution of surface conduction for each column (Eq. [8]).

## Results

The results of the parameter estimation conducted using Hydrus 1-D for the multi-step outflow experiment are presented in Table 3.

**Table 3)** Hydrus-1D inverse solution showing parameter estimation and standard error for Column 1 (a) and Column 2 (b)

Experimental Parameter	(a)		(b)	
	Value	Standard Error	Value	Standard Error
$\alpha_1$	0.70	0.31	0.68	0.17
$N_1$	1.74	0.36	3.32	1.30
$K_s$	0.17	0.02	56.07	19.43
$w_2$	0.67	0.04	0.86	0.01
$\alpha_2$	$4.28 \times 10^{-3}$	$1.67 \times 10^{-3}$	0.01	$1.29 \times 10^{-3}$
$N_2$	1.42	0.12	1.29	0.02

The dual porosity inverse solutions for Columns 1 and 2 achieved  $R^2$  of 94.9% and 98.9% and mass balance error of 0.0915% and 0.0860%, respectively. Using these parameters, the moisture content at the plane of IP measurement was determined by using the Durner

equation (Eq. [12]) and measured tensions ( $h$ ) (Figure 3).

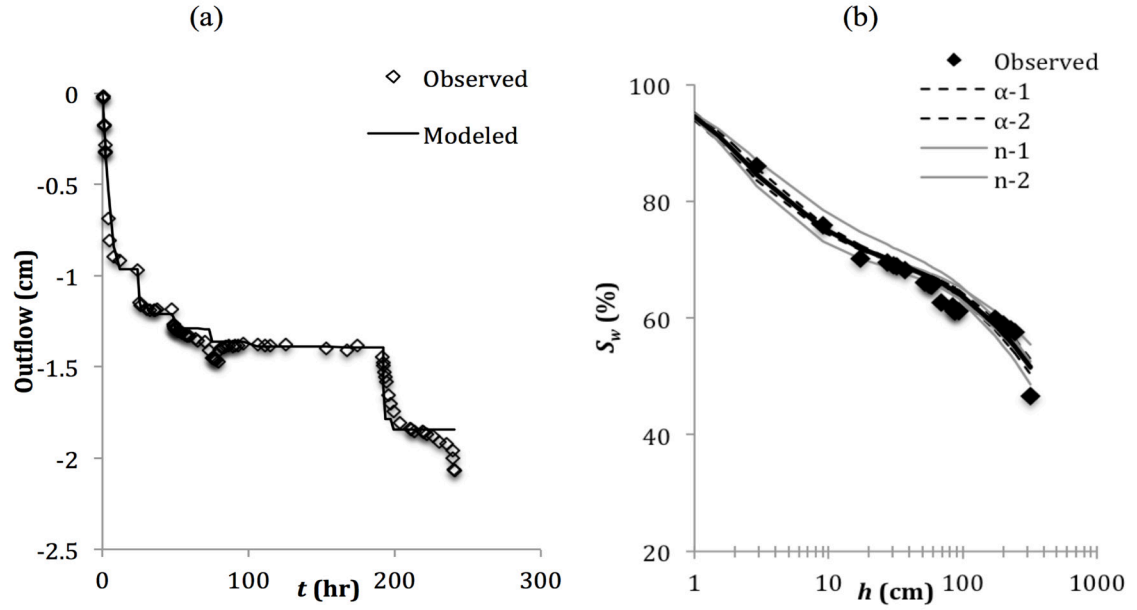


**Figure 3)** (a) Observed outflow versus Hydrus modeled outflow, (b) Observed average water content and modeled water content at lower tensiometers including sensitivity analysis varying estimated parameters ( $\alpha-1$ ,  $\alpha-2$ ,  $n-1$  and  $n-2$ ) by  $\pm 10\%$  in Column 1 No Flow.

During desaturation the modeled water content shows variation with observed average water content at times showing higher and lower values. The maximum variation between modeled water content and observed water content is approximately 4% saturation. To determine the contribution of each parameter, a sensitivity analysis was conducted by varying the modeling parameters  $\alpha$  and  $N$  for both pore systems. This sensitivity analysis is additionally shown on Figure 3b. The sensitivity analysis shows that the lack of fit observed at the end of the outflow experiments is not a result of the poor fit rather, the inability of the model to fully capture the dynamics observed in the

column.

Figure 4 presents the IP response for Columns 1 and 2 during flow and no flow conditions versus the modeled water content, where  $\sigma'$  is seen to initially increase, and then decrease with decreasing saturation; in contrast,  $\sigma''$  overall decreases with water content.

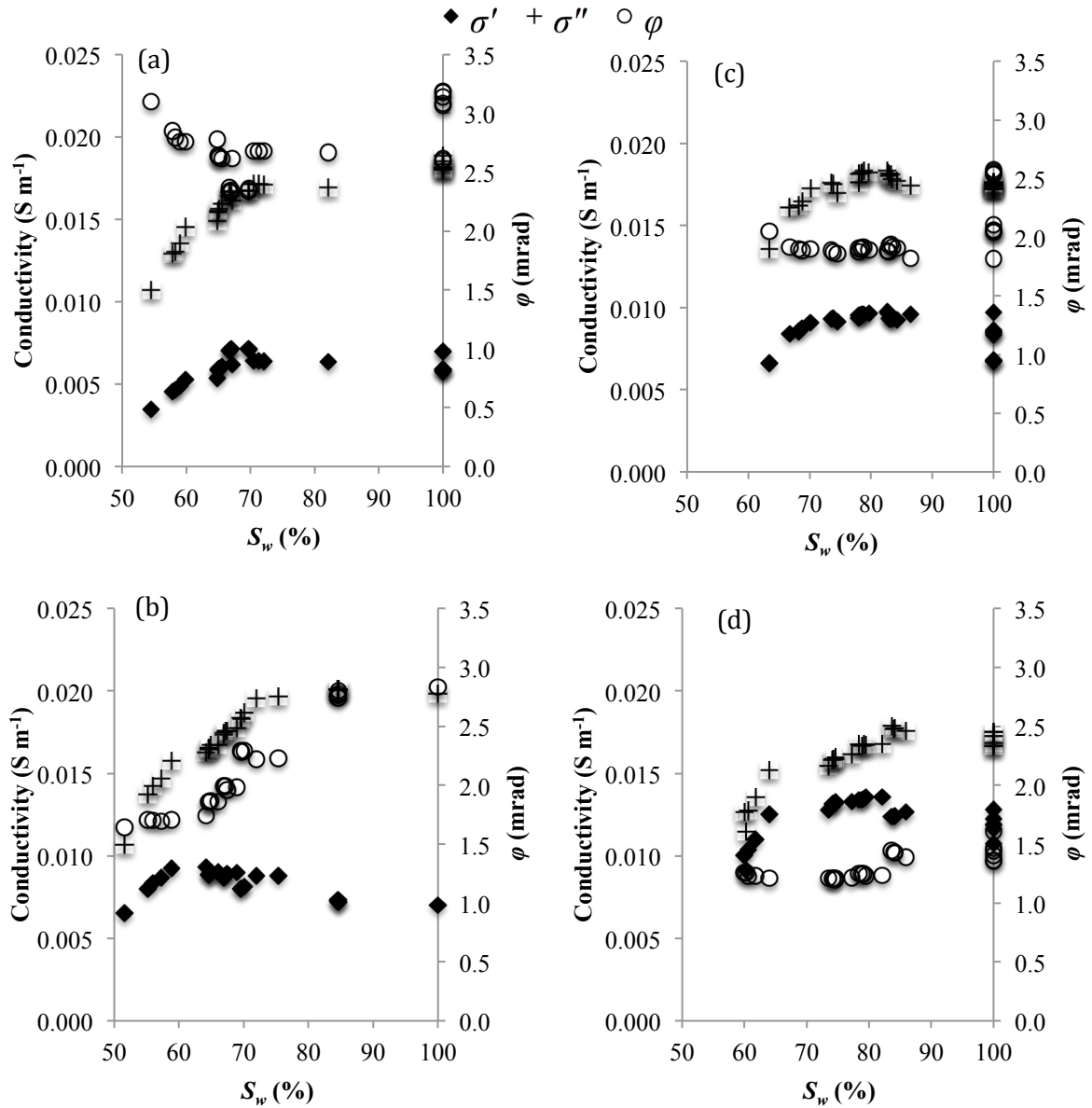


**Figure 4)** IP results at 1 Hz during multi-step outflow experiment showing real conductivity ( $\sigma'$ ), imaginary conductivity ( $\sigma''$ ) and phase shift ( $\phi$ ) for Column 1 Flow (a),

Column 1 No Flow (b), Column 2 Flow (c), and Column 2 No Flow (d), imaginary conductivity scaled by 1000.

No characteristic peak frequency typical of a dominant grain size or pore length (Kormiltsev, 1963; Schwarz, 1962) was detected in the soil likely due to the superposition of peaks associated with the heterogeneous nature of our soil (Figure 5).

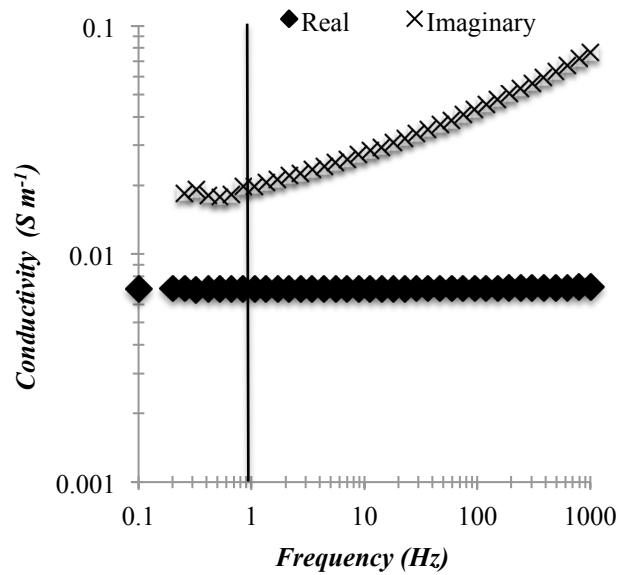


**Figure 5)** SIP results for Column 1 during multi-step outflow experiment showing frequency dependence of real conductivity ( $\sigma'$ ) and imaginary conductivity ( $\sigma''$ ) and line indicating 1 Hz frequency used for single frequency analysis, imaginary conductivity scaled by 1000

$\sigma'$  is unaffected by frequency and  $\sigma''$  increases slightly with frequency. As no characteristic peak in frequency is observed in the  $\sigma''$  results, we focus our analysis on the single frequency of 1 Hz.

### **Real Conductivity**

The results of the Archie experiment are presented in Figure 6. The formation factor was determined to be  $5.9 \pm 0.5$  and  $7.7 \pm 0.6$  for Columns 1 and 2, respectively. Surface conduction was determined to be  $0.0007 \pm 0.0001 \text{ S m}^{-1}$  for both Columns 1 and 2. Using the determined formation factor, Archie's cementation factor was determined to be 1.83 and 2.03 for Columns 1 and 2 respectively (Eq. [7]). In addition to determining the surface conduction and formation factor, we additionally observed an increase of  $15 \mu\text{S cm}^{-1}$  in the outflow fluid during percolation of deionized water associated with the release of ions from the soil.

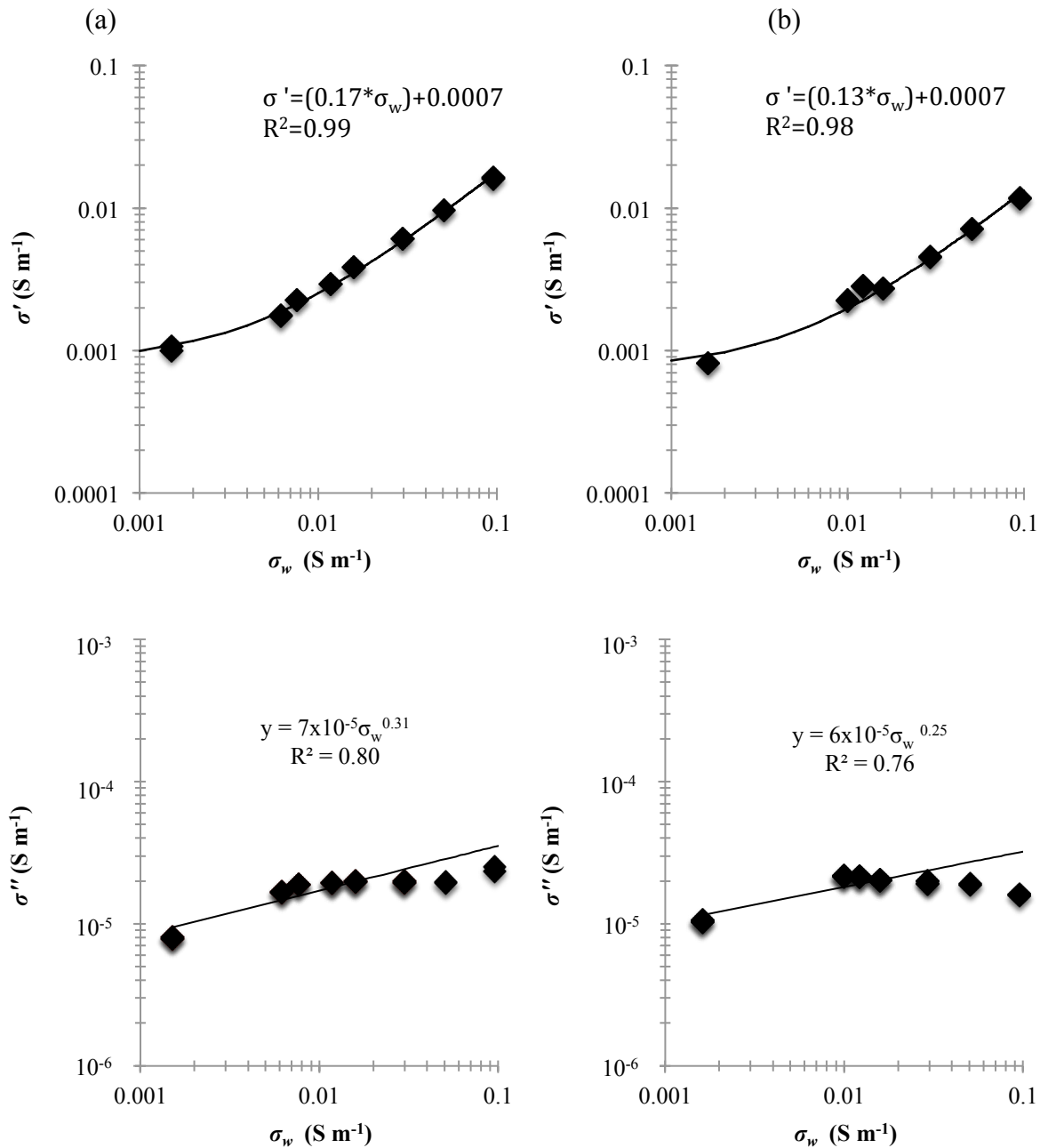


**Figure 6)** Real ( $\sigma'$ ) and Imaginary Conductivity ( $\sigma''$ ) versus pore fluid conductivity ( $\sigma_w$ ) showing a linear relationship for real conductivity in Column 1 (a) and Column (2) (b) and a weaker dependence of imaginary conductivity

To evaluate the  $\sigma'$  response, a fitting was first attempted for  $n$  using the experimentally determined parameters from the Archie experiment (Figure 7). However, due to the increase in pore fluid conductivity  $\sigma_w$  observed in the outflow, a simple fitting was not possible (Eq. [10]). The fitting resulted in non-convergence at the lower limit of  $n$  at 1. The small volume of fluid collected throughout each outflow interval prevented reliable measurements of the outflow conductivity. However,  $\sigma'$  was not seen to obey a power law decrease with decreases in saturation, but rather was seen to initially increase followed by a decrease. An increase of  $\sigma_w$  during the experiment could result from different mechanisms, such as release from an ion source or evaporation. To account for this behavior, pore fluid conductivity was modified in Archie's equation (Eq. [10]) using a general form of a polynomial equation to account for release of ions as a nonlinear function of time ( $t$ ) into the pore water:

$$\sigma_w = l t^k + \sigma_o \quad (14)$$

where  $l$  is a lumped fitting parameter,  $k$  is the exponent of ion release, and  $\sigma_o$  is the initial conductivity of the input solution. In this equation, different exponents can occur depending on the type of process causing the conductivity increase. For first order kinetic release processes the exponent is 1, for film diffusion exponents it can range between 0 and 1, for diffusion the exponent is typically 0.5, and finally for time variable diffusion or processes near equilibrium exponents can be smaller than 0.5 (Kookana et al., 1992; Wehrer et al., 2012). Using this ion release relationship and the previously discussed assumption that available surfaces for conduction decrease during desaturation (Eq. [10])

we fit the data with:

$$\sigma' = [(lt^k + \sigma_o)\varphi^m S_w^n] + \sigma'_{surf} S_w^p \quad (15)$$

where  $l$ ,  $k$ , and  $n$  were fitting parameters. The results of this fitting are presented in Table 4.

**Table 4)** Parameter estimation for real conductivity accounting for ion release (Eq. [18]) and no ion release (Eq. [10]) for Column 1 no flow (a) and Column 2 no flow (b) with root mean square errors (RMSE)

	(a)	(b)
<b>Experimental Parameter</b>	<b>Value</b>	<b>Value</b>
$l$ †	0.052	0.054
$k$	0.31	0.26
$C_o$	0.038	0.038
$\Phi$	0.36	0.36
$m$	1.83	2.03
$n$ †	1.74	1.00
$\sigma'_{surf}$	0.0007	0.0007
$RMSE$	0.001	0.001
$C_o$	0.038	0.038
$\Phi$	0.36	0.36
$m$	1.83	2.03
$n$ †	1.00	1.00
$\sigma'_{surf}$	0.0007	0.0007
$RMSE$	0.004	0.008

† Fitted Parameter

A representative fitting with and without release of ions for Column 1 during no flow conditions is presented in Figure 7. Fitting relationship Eq. [15] based on minimizing the root mean square error (RMSE) explains the data very well for no flow conditions. The non-smooth result of the fitting is due to the non-linear and discontinuous relationship



between time and saturation, due to the sudden changes of the suction boundary condition.

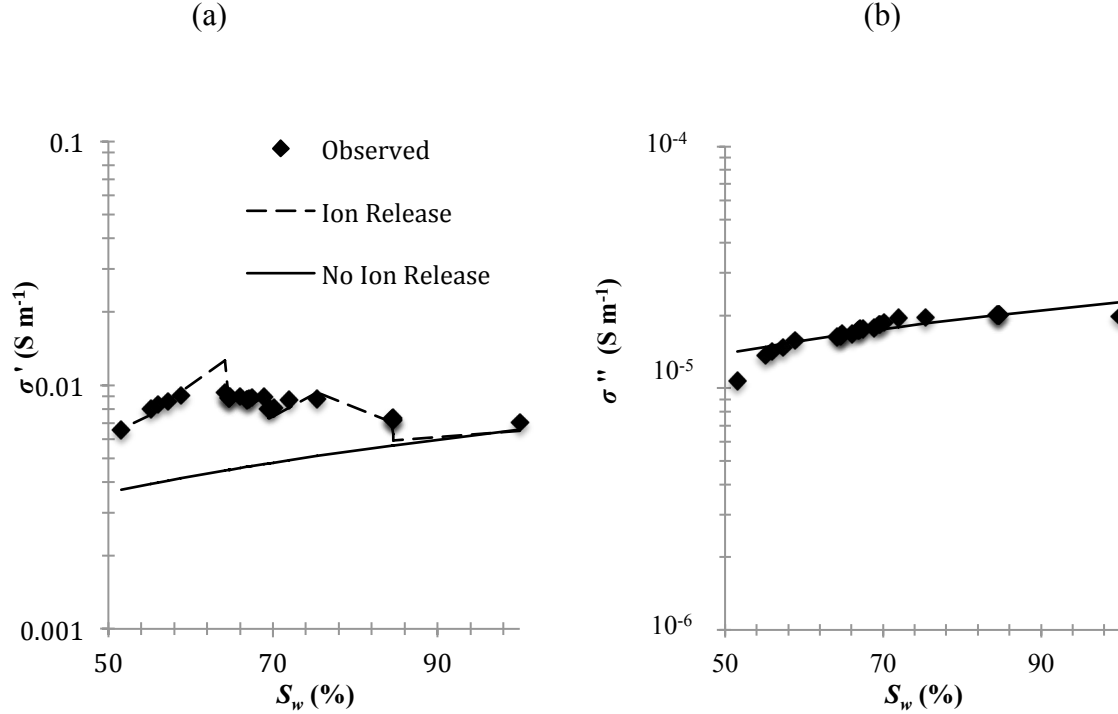


**Figure 7)** (a) Real conductivity ( $\sigma'$ ) versus saturation showing modeled fits accounting for ion release and not accounting for ion release using constant pore fluid conductivity in Column 1 during no flow conditions. (b) Imaginary conductivity ( $\sigma''$ ) versus saturation in Column 1 during no flow conditions showing a power law relationship.

We refrained from fitting the model for the experiment under flow conditions, because of the multiple interdependent processes that will operate during flow. Due to the continuous exchange of pore fluid and the presence of a dual porosity, consisting of both mobile and immobile pore fluids, we assume that Eq. [15] is not able to correctly represent the processes of pore fluid conductivity during flow conditions.

### Imaginary Conductivity

While  $\sigma'$  varied over three orders of magnitude with changes in salinity,  $\sigma''$  demonstrated a much weaker salinity dependence (Figure 6) during the saturated Archie experiment. A power law relationship was fit to the data, to compare our results to those of Weller and Slater (2012). Similar to Weller and Slater (2012), we observed power law exponents of approximately 0.3 below  $30 \text{ mS m}^{-1}$  and we see evidence of the asymptotic zone with further increases in pore fluid conductivity (Figure 6b). This weak dependence on fluid chemistry is highlighted in our columns under unsaturated conditions as the general response of  $\sigma''$  for both columns during flow and no flow conditions exhibited essentially the same response (Figure 8).

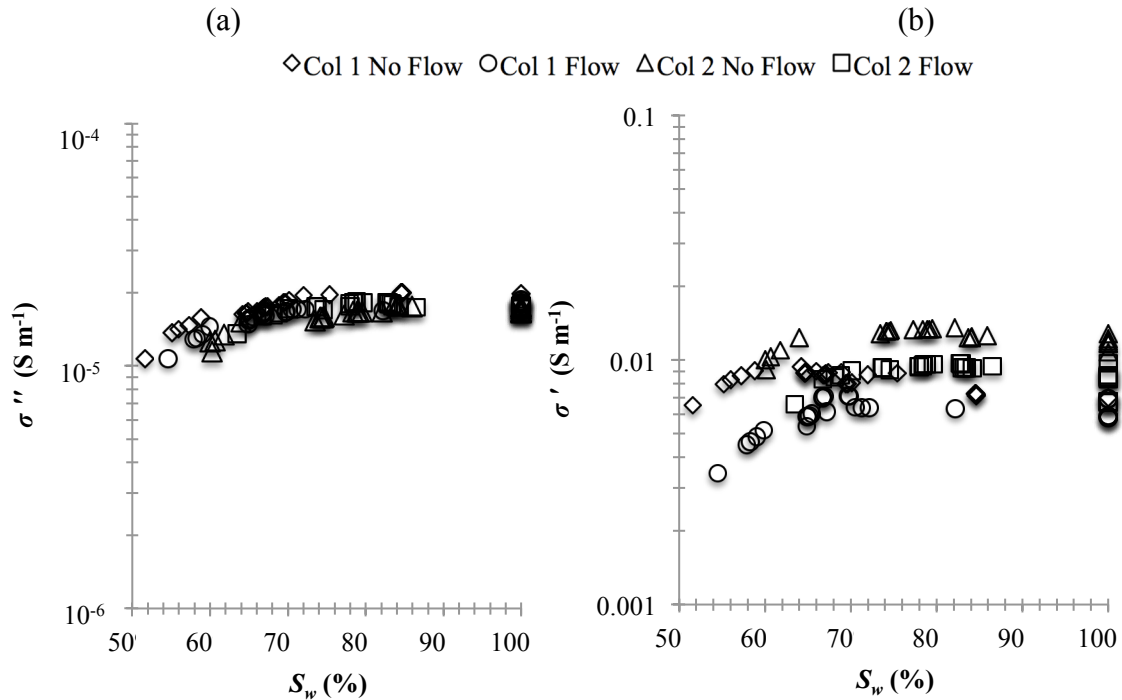


**Figure 8)** Similarity between imaginary conductivities ( $\sigma''$ ) versus saturation in all four datasets with power law relationship shown (a) compared to dissimilarities between real conductivities ( $\sigma'$ ) versus saturation in all four datasets (b)

Also, the initial increase followed by a decrease as observed for the  $\sigma''$  was not present. To describe the relationship of  $\sigma''$  and saturation, we fit our data using a power law equation previously discussed (Eq. [9]). To fit this, we fit  $\sigma''$  as a function of saturation with both  $a$  and  $p$  as fitting parameters (Table 5).

**Table 5)** Parameter estimation for power law relationship of imaginary conductivity with saturation (Eq. [9]) for Column 1 no flow (a) and Column 2 no flow (b)

	(a)	(b)
Experimental Parameter	Value	Value
$a$ *	$2.26 \times 10^{-5}$	$4.32 \times 10^{-7}$
$p$ *	0.71	0.83
$R^2$	77%	83%

\* fitted parameter

In column 1 the fitting does closely match the relationship described by Vinegar and Waxman (1984) of  $p=n-1$ . This same relationship is not present in column 2 as  $n=1$ . As shown by Figure 7, the data follows a power law relationship observed by Ulrich and Slater (2004) and Su et al. (2000).

## Discussion

While many other researchers have compared electrical results to average water content, this may not account for a gradient of moisture content throughout the sampling volume. Additionally, using a traditional vertical electrode geometry this gradient would cause the IP measurements to be collected over a range of moisture contents. To mitigate these potential errors, we have presented measurements on a column experiment where soil

hydraulic data were concurrently measured with electrical resistivity and IP data under flow and no flow conditions in a horizontal plane. Using these data we were able to create an inverse model using Hydrus 1-D to model the water retention curves for each column. A large variation in  $K$  was present between the two columns, which could possibly be attributed to a macropore in column 2. Using the estimated parameters (Table 3) and the Durner equation (Eq. [12]) we were able to use the observed tension measured with each tensiometer ( $h$ ) to predict water contents ( $S_w$ ) along the plane of measurement. In general a variation of modeled water content and observed average water content was present; however, the maximum variation is a difference of 4% (Figure 3). We assume that this model misfit can be attributed to structural deficits of the model, which may either originate from the use of a parameter based water retention curve or to non-equilibrium conditions. Nevertheless, the model gives a good representation of the water content dynamics at the plane of measurement with small deviations between average water content and modeled water content. We consider these water content estimates sufficient for our purpose. These modeling results show that average water contents are a sufficient approximation, if it is aimed for a relationship between complex conductivity and saturation in short soil columns. However, care should be taken if averaging is performed over longer columns.

We found  $\sigma'$  and  $\sigma''$  to exhibit general decreases with decrease in soil saturation consistent with previous studies. While variation is present in the fitted  $n$  values for  $\sigma'$ , they are within the range previously reported by others. We showed that  $\sigma'$  demonstrated a complex saturation dependence that was affected by not only moisture content

decreases but also by an increase of pore fluid conductivity. Several factors likely contributed to the increase of pore fluid conductivity. These factors may be evaporation, release of ions from the soil matrix, temperature increases in the measurement environment, and release of ions from electrodes. Evaporation could cause significant increases in pore fluid salinity. While we are unable to directly measure the effects of evaporation, we assume this process to be negligible because the top of the column was covered during the outflow experiment. An increase in the temperature of the laboratory environment may result in increases in conductivity; however, the laboratory was temperature controlled and no such increases were measured during the experiment. Release of ions from the electrodes is quite plausible due to the direct connection of the electrolyte solution to the soil. To check this theory a simple diffusion test was conducted by placing a single electrode in a 100 mL beaker of deionized water and measuring conductivity as a function of time. This test showed a power law increase in fluid salinity with an exponent of 0.5 consistent with diffusion. Finally, the soil itself likely released ions due to mineral dissolution and desorption. We are unable to differentiate the contributions of the electrodes and the ion release from the soil matrix.

During experimental design, we planned on collecting measurements under flow conditions to avoid the effects of the release of ions but this could not fully be avoided due to the low flow velocities achieved. To account for the increase of pore fluid conductivity we modeled the results using an empirical polynomial equation accounting for a time dependent release of ions. The fitted exponent is smaller than 0.5, suggesting either a time dependent diffusion coefficient or near equilibrium conditions (Wehrer et

al., 2012). A time dependent diffusion coefficient could occur when the porous cups become clogged, for example by air bubbles or soil colloidal material.

For  $\sigma''$ , we did not observe a peak value at a specific saturation as discussed by Titov et al. (2004) and observed by Ulrich and Slater (2004) during pressure drainage. This may relate to the heterogeneous grain size distribution of our soil column, which creates a range of pore sizes. Unlike for a uniform grain size distribution, different ratios of large to narrow water filled pore diameters will exist simultaneously at all times during desaturation. This would result in a smoothing out of the peak saturation responses of  $\sigma''$ . Such a response was also reported by Ulrich and Slater (2004) during their evaporative drying cycle; this again might be expected as evaporation results in a more uniform removal of water from all pores. Schmutz et al. (2010) additionally did not see this peak response. Alternatively, the saturation response of  $\sigma''$  may not be controlled by the ratio of large and narrow water filled pore diameters as presented by Titov et al. (2002), but rather be controlled by the polarization of the Stern layer discussed by Jougnot et al. (2010). As shown in Figure 7b, a power law relationship described by Jougnot et al. (2010) does not perfectly describe our results as shown by the inadequacy of the fit, which may be the effect of increasing salinity. A complex  $\sigma'$  behavior during desaturation of the columns was observed due to a strong dependency on salinity. In contrast, the dependency of  $\sigma''$  on salinity was much weaker. In fact, the  $\sigma''$  response observed between both columns during flow and no flow conditions was essentially the same (Figure 8), which indicates  $\sigma''$  was controlled primarily by changes in saturation despite the changes in salinity that were occurring.

Previous studies have conducted similar experiments to what is presented here (Breede et al., 2011; Revil et al., 2011; Titov et al., 2004; Ulrich and Slater, 2004); however, to our knowledge these previous studies have not accounted for the potential variation in pore fluid conductivity when modeling  $\sigma'$ , but instead have kept pore fluid conductivity constant in Archie's equation. Disregarding the potential for pore fluid changes in resistivity surveys will likely result in a poor determination of moisture content as, when these measurements are conducted in the field, pore fluid conductivity changes are likely to occur simultaneously with water content changes. Such changes may occur due to a wider range of natural processes, such as mineral dissolution, ion exchange and evaporation or due to anthropogenic influences such as fertilizer addition. As these changes are practically impossible to directly measure over a spatial extent, the accurate determination of salinity contributions and moisture content are unable to be made without additional information. As  $\sigma''$  is shown to be relatively independent of salinity changes compared to changes in saturation, this work suggests that IP may be a valuable tool in conducting hydraulic investigations and may hold the key to hydraulic determinations in geophysical investigations. Larger scale studies utilizing IP and electrical resistivity are thus required to determine whether induced polarization does give better information than electrical resistivity alone.

## **Conclusion**

Electrical methods including electrical resistivity and IP provide a unique opportunity to measure in-situ spatial variations of soil physical properties, which previously could only be measured using point measurement tools. By conducting IP measurements we showed

that although  $\sigma''$  dependence on saturation is weaker than  $\sigma'$ ,  $\sigma''$  provides a more robust determination of saturation in the presence of changing salinities. Further experiments on different soil types would be advantageous to determine if this relationship holds and additionally further studies beyond 1-D columns would be needed to see if this relationship could be used for saturation determinations over a spatial extent.

## References

- Archie, G.E., 1942. The electrical resistivity log as an aid in determining some reservoir characteristics. *T Am Inst Mineral Metall Petrol Eng* 146, 54–62.
- Binley, A., Winship, P., West, L.J., Pokar, M., Middleton, R., 2002. Seasonal variation of moisture content in unsaturated sandstone inferred from borehole radar and resistivity profiles. *Journal of Hydrology* 267, 160-172.
- Blume, H.P., Brümmer, G.W., Horn, R., Kandeler, E., Kögel-Knabner, I., Kretzschmar, R., Stahr, K., Wilke, B.M., Schachtschabel, P., 2010. Scheffer/Schachtschabel: *Lehrbuch der Bodenkunde*. Spektrum Akademischer Verlag.
- Bodmer, R., Ward, S.H., Morrison, H.F., 1968. On induced electrical polarization and groundwater. *Geophysics* 33, 805-821.
- Börner, F., 1991. Untersuchungen zur komplexen elektrischen Leitfähigkeit von Gesteinen im Frequenzbereich von 1 Millihertz bis 10 Kilohertz, Bergakademie Freiberg, Germany.
- Börner, F., 1992. Complex conductivity measurements of reservoir properties, *Proc Third European Core Analysis Symposium*, Paris, pp. 359-386.
- Breede, K., Kemna, A., Esser, O., Zimmermann, E., Vereecken, H., Huisman, J.A., 2011. Joint Measurement Setup for Determining Spectral Induced Polarization and Soil Hydraulic Properties. *Vadose Zone Journal* 10, 716-726.
- Cassiani, G., Dalla, E., Brovelli, A., Pitea, D., 2004. Pore-scale modeling of electrical conductivity in unsaturated sandstones. *Developments in Water Science* 55, 235-245.
- Clothier, B.E., Green, S.R., Deurer, M., 2008. Preferential flow and transport in soil;



progress and prognosis. *European Journal of Soil Science* 59, 2-13.

Cole, K.S., Cole, R.H., 1941. Dispersion and Absorption in Dielectrics I. Alternating Current Characteristics. *The Journal of Chemical Physics* 9, 341-351.

Cosenza, P., Ghorbani, A., Florsch, N., Revil, A., 2007. Effects of Drying on the Low-Frequency Electrical Properties of Tournemire Argillites. *Pure and Applied Geophysics* 164, 2043-2066.

Darcy, H., 1856. Les fontaines publiques de la ville de Dijon. Exposition et application des principes à suivre et des formules à employer dans les questions de distribution d'eau: ouvrage terminé par un appendice relatif aux fournitures d'eau de plusieurs villes au filtrage des eaux et à la fabrication des tuyaux de fonte, de plomb, de toile et de bitume. Dalmont.

Durner, W., Priesack, E., Vogel, H.J., Zurmühl, T., 1999. Determination of parameters for flexible hydraulic functions by inverse modeling. *Workshop on Characterization and measurement of the hydraulic properties of unsaturated porous media*, 817-829.

Eleraki, M., Gadallah, M.M., Gemal, K.S., Attwa, M., 2010. Application of resistivity method in environmental study of the appearance of soil water in the central part of Tenth of Ramadan City, Egypt. *Quarterly Journal of Engineering Geology and Hydrogeology* 43, 171-184.

Ewing, R.P., Hunt, A.G., 2006. Dependence of the Electrical Conductivity on Saturation in Real Porous Media. *Vadose Zone Journal* 5, 731-741.

Flath, D., 1989. The low-frequency complex electrical response of brine-saturated shaly sandstones, University of Birmingham.

Franz, T.E., Nolan, J., Nordbotten, J.M., Caylor, K.K., Slater, L.D., 2011. Quantifying Transient Soil Moisture Dynamics Using Multipoint Direct-Current Resistivity in Homogeneous Sand. *Vadose Zone Journal* 10, 286-298.

French, H., Binley, A., 2004. Snowmelt infiltration: monitoring temporal and spatial variability using time-lapse electrical resistivity. *Journal of Hydrology* 297, 174-186.

Frye, K.M., Lesmes, D.P., Morgan, F.D., 1998. The influence of pore fluid chemistry on the induced polarization response of rocks and soils, *Proceedings of the Symposium on the Application of Geophysics to Engineering and Environmental Problems*, pp. 1-780.

- Garre, S., Koestel, J., Gunther, T., Javaux, M., Vanderborght, J., Vereecken, H., 2010. Comparison of Heterogeneous Transport Processes Observed with Electrical Resistivity Tomography in Two Soils. *Vadose Zone Journal* 9, 336-349.
- Ghorbani, A., Cosenza, P., Revil, A., Zamora, M., Schmutz, M., Florsch, N., Jougnot, D., 2009. Non-invasive monitoring of water content and textural changes in clay-rocks using spectral induced polarization; a laboratory investigation. *Applied Clay Science* 43, 493-502.
- Glover, P., 1998. Nature of surface electrical conductivity sandstones, and clays. *Geophysical Research Letters* 25, 691-694.
- Hillel, D., 2004. *Introduction to Environmental Soil Physics*. Academic Press, USA.
- Hubbard, S.S., Rubin, Y., 2000. Hydrogeological parameter estimation using geophysical data: a review of selected techniques. *Journal of Contaminant Hydrology* 45, 3-34.
- Jarvis, N.J., 2007. A review of non-equilibrium water flow and solute transport in soil macropores: principles, controlling factors and consequences for water quality. *European Journal of Soil Science* 58, 523-546.
- Jougnot, D., Ghorbani, A., Revil, A., Leroy, P., Cosenza, P., 2010. Spectral induced polarization of partially saturated clay-rocks: a mechanistic approach. *Geophysical Journal International* 180, 210-224.
- Kemna, A., Binley, A., Ramirez, A., Daily, W., 2000. Complex resistivity tomography for environmental applications. *Chemical Engineering Journal* 77, 11-18.
- Kookana, R.S., Aylmore, L., Gerritse, R., 1992. Time-dependent sorption of pesticides during transport in soils. *Soil science* 154, 214-225.
- Kormiltsev, V., 1963. O возбужdenii i spade vyzvannoi polarizatsii v kapillarnoi srede (On excitation and decay of induced polarization in capillary medium). *Izvestia AN SSSR, Seria Geofizicheskaya (Solid Earth Physics)* 11, 1658-1666.
- Lesmes, D., Friedman, S., 2005. Relationships between the Electrical and Hydrogeological Properties of Rocks and Soils, in: Rubin, Y., Hubbard, S. (Eds.), *Hydrogeophysics*. Springer Netherlands, pp. 87-128.
- Liu, S., Yeh, T.-C.J., 2004. An Integrative Approach for Monitoring Water Movement in the Vadose Zone. *Vadose Zone Journal* 3, 681-692.

Maineult, A., Bernab, Y., Ackerer, P., 2004. Electrical Response of Flow, Diffusion, and Advection in a Laboratory Sand Box. *Vadose Zone Journal* 3, 1180-1192.

McLaughlin, M.J., 1982. A Review of the Use of Dyes as Soil Water Tracers. *Water SA* 8, 6.

Mitchell, V., Knight, R., Pidlisecky, A., 2011. Inversion of time-lapse electrical resistivity imaging data for monitoring infiltration. *The Leading Edge* 30, 140-144.

Nordsiek, S., Weller, A., 2008. A new approach to fitting induced-polarization spectra. *Geophysics* 73, F235-245.

Revil, A., Florsch, N., 2010. Determination of permeability from spectral induced polarization in granular media. *Geophysical Journal International* 181, 1480-1498.

Revil, A., Schmutz, M., Batzle, M.L., 2011. Influence of oil wettability upon spectral induced polarization of oil-bearing sands. *Geophysics* 76, A31-A36.

Revil, A., Schwaeger, H., Cathles, L.M., Manhardt, P.D., 1999. Streaming potential in porous media: 2. Theory and application to geothermal systems. *Journal of Geophysical Research: Solid Earth* 104, 20033-20048.

Richards, L.A., 1931. Capillary conduction of liquids through porous mediums. *Physics* 1, 318-333.

Samoulian, A., Cousin, I., Tabbagh, A., Bruand, A., Richard, G., 2005. Electrical resistivity survey in soil science: a review. *Soil and Tillage Research* 83, 173-193.

Schmutz, M., Revil, A., Vaudelet, P., Batzle, M., Vinao, P.F., Werkema, D.D., 2010. Influence of oil saturation upon spectral induced polarization of oil-bearing sands. *Geophysical Journal International* 183, 211-224.

Schön, J.H., 2004. *Physical Properties of Rocks: Fundamentals and Principles of Petrophysics*. Elsevier Science Limited.

Schwarz, G., 1962. A Theory of the Low-Frequency Dielectric Dispersion of Colloidal Particles in Electrolyte Solution<sup>1,2</sup>. *The Journal of Physical Chemistry* 66, 2636-2642.

Seigel, H.O., 1959. Mathematical formulation and type curves for induced polarization. *Geophysics* 24, 547-565.

Sharma, P.V., 1997. Environmental and Engineering Geophysics. Cambridge University Press, Cambridge, UK; New York, NY USA.

Šimůnek, J., van Genuchten, M.T., Šejna, M., 2008. Development and Applications of the HYDRUS and STANMOD Software Packages and Related Codes. *Vadose Zone Journal* 7, 587-600.

Slater, L., 2007. Near surface electrical characterization of hydraulic conductivity: From petrophysical properties to aquifer geometries - A review. *Surv. Geophys.* 28, 169-197.

Slater, L.D., Glaser, D.R., 2003. Controls on induced polarization in sandy unconsolidated sediments and application to aquifer characterization. *Geophysics* 68, 1547-1558.

Slater, L.D., Lesmes, D., 2002. IP interpretation in environmental investigations. *Geophysics* 67, 77-88.

Su, Q., Feng, Q., Shang, Z., 2000. Electrical impedance variation with water saturation in rock. *Geophysics* 65, 68-75.

Titov, K., Kemna, A., Tarasov, A., Vereecken, H., 2004. Induced Polarization of Unsaturated Sands Determined through Time Domain Measurements. *Vadose Zone Journal* 3, 1160-1168.

Titov, K., Komarov, V., Tarasov, V., Levitski, A., 2002. Theoretical and experimental study of time domain-induced polarization in water-saturated sands. *Journal of Applied Geophysics* 50, 417-433.

Ulrich, C., Slater, L.D., 2004. Induced polarization measurements on unsaturated, unconsolidated sands. *Geophysics* 69, 762-771.

van Genuchten, M.T., 1980. A Closed-form Equation for Predicting the Hydraulic Conductivity of Unsaturated Soils<sup>1</sup>. *Soil Sci. Soc. Am. J.* 44, 892-898.

Vereecken, H., Kaiser, R., Dust, M., Pütz, T., 1997. Evaluation of the multistep outflow method for the determination of unsaturated hydraulic properties of soils. *Soil science* 162, 618-631.

Vinegar, H.J., Waxman, M.H., 1984. Induced polarization of shaly sands. *Geophysics* 49, 1267-1287.

Waxman, M.H., Smits, L.J.M., 1968. Electrical conductivities in oil-bearing shaly sands. SPEJ. Society of Petroleum Engineers Journal 8, 107-122.

Wehrer, M., Mai, J., Attinger, S., Totsche, K.U., 2012. Kinetic control of contaminant release from NAPLs – information potential of concentration time profiles (Submitted). Environmental Pollution.

Wehrer, M., Totsche, K.U., 2009. Difference in PAH release processes from tar-oil contaminated soil materials with similar contamination history. Chemie der Erde-Geochemistry 69, 109-124.

Weller, A., Breede, K., Slater, L., Nordsiek, S., 2011. Effect of changing water salinity on complex conductivity spectra of sandstones. Geophysics 76, F315-327.

Weller, A., Slater, L., 2012. Salinity dependence of complex conductivity of unconsolidated and consolidated materials: Comparisons with electrical double layer models. Geophysics 77, D185-D198.

Weller, A., Slater, L., Nordsiek, S., Ntarlagiannis, D., 2010. On the estimation of specific surface per unit pore volume from induced polarization: A robust empirical relation fits multiple data sets. Geophysics 75, WA105-112.

Wenner, F., 1916. A method of measuring earth resistivity. Electric Prospecting 12, 469-478.

## Curriculum vitae

David A Grunat

### **Birth**

Born April 4, 1985

Beach Grove, Indiana

### **Education**

**Carmel High School** –Carmel, IN 1999-2000

**University High School**- Carmel, IN 2000-2003

**Indiana University**-Bloomington, IN 2003-2007

**Bachelor of Science in Environmental Science – Hydrology/Water Resources**

### **Professional Experience**

**Field Technician; Indiana Geological Survey**, Bloomington, IN 2006-2007

**Conestoga-Rovers and Associates**, Emeryville, CA 2008-2011

Project Manager (2010-2011);

Staff Geologist (2009-2010);

Remediation Technician (2008-2009)

**Project Geologist; Fleming-Lee Shue**, New York, NY 2011-2012

**Environmental Consultant; Self Employed**, New York, NY 2011- Present